

Orbital excitation blockade and algorithmic cooling in quantum gases

Waseem S. Bakr, Philipp M. Preiss, M. Eric Tai, Ruichao Ma, Jonathan Simon, and Markus Greiner
Department of Physics, Harvard University, Cambridge, Massachusetts, 02138, USA

(Dated: October 30, 2018)

Interaction blockade occurs when strong interactions in a confined few-body system prevent a particle from occupying an otherwise accessible quantum state. Blockade phenomena reveal the underlying granular nature of quantum systems and allow the detection and manipulation of the constituent particles, whether they are electrons[1], spins[2], atoms[3–5], or photons[6]. The diverse applications range from single-electron transistors based on electronic Coulomb blockade[7] to quantum logic gates in Rydberg atoms[8, 9]. We have observed a new kind of interaction blockade in transferring ultracold atoms between orbitals in an optical lattice. In this system, atoms on the same lattice site undergo coherent collisions described by a contact interaction whose strength depends strongly on the orbital wavefunctions of the atoms. We induce coherent orbital excitations by modulating the lattice depth and observe a staircase-type excitation behavior as we cross the interaction-split resonances by tuning the modulation frequency. As an application of orbital excitation blockade (OEB), we demonstrate a novel algorithmic route for cooling quantum gases. Our realization of algorithmic cooling[10, 11] utilizes a sequence of reversible OEB-based quantum operations that isolate the entropy in one part of the system, followed by an irreversible step that removes the entropy from the gas. This work opens the door to cooling quantum gases down to ultralow entropies, with implications for developing a microscopic understanding of strongly correlated electron systems that can be simulated in optical lattices[12, 13]. In addition, the close analogy between OEB and dipole blockade in Rydberg atoms provides a roadmap for the implementation of two-qubit gates[14] in a quantum computing architecture with natural scalability.

An ultracold gas of bosonic atoms in the ground band of an optical lattice is described by the Bose-Hubbard model[15], in which atoms can tunnel between neighboring sites and interact via an onsite repulsive contact interaction. In a deep lattice where the interactions dominate, the ground state of the system is a Mott insulator with a fixed atom number per site that is locally constant over a region of the insulator[16]. The energy per site in the absence of tunneling is $\frac{1}{2}U_{gg}n(n-1)$, where U_{gg} is the interaction energy for two atoms in the ground lattice orbital state and n is the atom number on the site. The Mott state exhibits a transport blockade phenomenon in which the presence of an atom on a site energetically prevents tunneling of a neighboring atom onto that site even in the presence of a small bias between the sites. The transport is blocked unless the bias makes up for the interaction cost, making it possible, for example, to count atoms tunneling across doublewells in a superlattice[3]. In this work, we explore an excitation blockade phenomenon that does not involve transport in the lattice. The excitation transfers localized atoms between different orbitals on the same site through modulation of the lattice depth at a frequency close to a vibrational resonance. Physics in higher optical lattice orbitals has been the focus of much recent experimental work including the study of dynamics in higher orbitals[17], multi-orbital corrections to the interaction energy[18], and unconventional forms of superfluidity involving higher orbitals[19, 20].

The OEB mechanism can be understood in the simplest scenario for two atoms in a single site of a deep three-dimensional lattice, in which the vibrational fre-

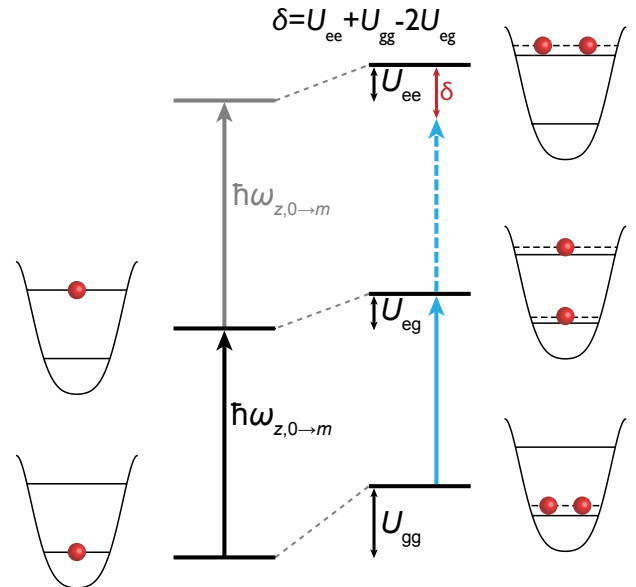


FIG. 1. Orbital excitation blockade mechanism in an optical lattice. A single atom on a site is excited to a higher orbital by resonantly modulating the lattice depth. For two atoms on the same site, interactions lead to an orbital-dependent energy shift. Modulation at the appropriate frequency excites one of the atoms to the higher orbital, but is off-resonant for exciting the second with a blockade energy δ .

quencies in all three directions are taken to be different to avoid degeneracies. The lattice depth along the z -direction is modulated weakly, which in the presence of anharmonicity of the lattice potential drives atoms between the ground orbital and a single, specific excited z -

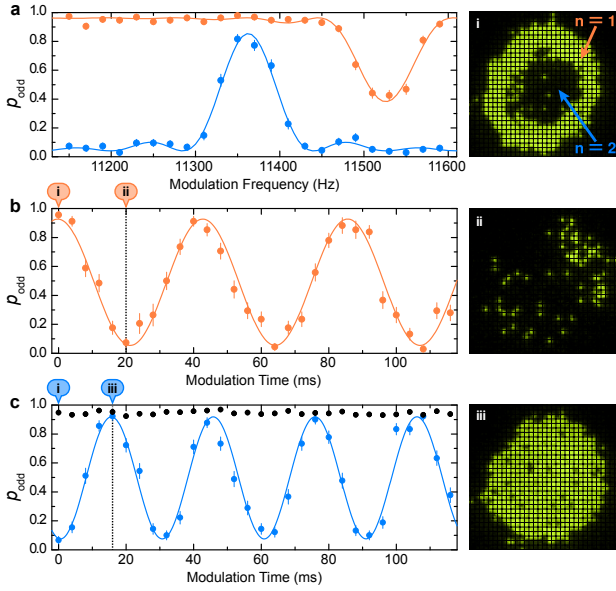


FIG. 2. Time, frequency and site-resolved coherent transfer of atoms in a Mott insulator between orbitals. **a**, Excitations transferring a single atom in the $n = 1$ (orange) or $n = 2$ shell (blue) from the ground to the second excited orbital are spectroscopically resolved in a two-shell Mott-insulator. **b**, Rabi oscillations between the two orbitals are observed by driving at the resonant frequencies for atoms in the $n = 1$ shell and **c**, $n = 2$ shell of a Mott insulator. Bose-enhancement leads to faster oscillations in the $n = 2$ shell. When the atom number is reduced to obtain one atom per site in the region previously containing two atoms, the interaction shift suppresses oscillations (black). All error bars are one standard error of the mean. **(i-iii)** Site-resolved snapshots of the Mott insulator are shown at different points in the Rabi cycles.

orbital, subject to a selection rule that only allows coupling to orbitals of the same symmetry. For a single atom, excitation to the m th orbital requires modulation at a frequency $\omega_{z,0 \rightarrow m}$ which is approximately $m\omega_{z,0 \rightarrow 1}$ ignoring the anharmonicity of the onsite potential. With more than one atom on a site, the interaction introduces an orbital-dependent shift of the energy levels as shown in Fig. 1. In general, the interaction shifts U_{gg} , U_{ge} , and U_{ee} are all different and the differences are a significant fraction of U_{gg} , where $g(e)$ denotes atoms in the ground (excited) orbital. If the coupling strength due to the modulation is small compared to these differences and the modulation frequency is tuned to $\omega_{z,0 \rightarrow m} + (U_{ge} - U_{gg})/\hbar$, only a single atom is transferred to the higher orbital and the transfer of a second atom is off-resonant. In this sense, the first excitation blocks the creation of a second excitation.

The experimental system has been described in previous work[21]. A two-dimensional Bose-Einstein condensate of rubidium atoms resides in a single plane of a one-dimensional optical lattice, henceforth referred to as the axial lattice, with a vibrational frequency of

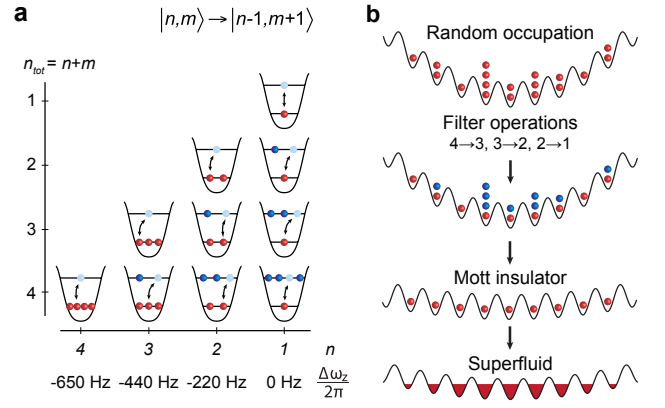


FIG. 3. Algorithmic cooling in an optical lattice. **a**, Landau-Zener chirp for transferring entropy from the ground to the fourth band. The lattice modulation frequency is swept across the transition resonances from left to right. The interaction shifts $\Delta\omega_z$ for excitation of one of n atoms to the fourth orbital relative to the excitation frequency for a single atom on a site, are shown for different orbital occupations. Excitation processes in the same column happen at almost the same frequency to within 30 Hz (see Supplementary Table I). **b**, A state with random occupation in a deep lattice is far from the Mott insulating ground state. Sequential filtering operations followed by reduction of the confinement prepares the ground state, which can be adiabatically converted to a thermalized superfluid in a shallow lattice. Red (blue) spheres denote atoms in the ground (excited) band.

$\omega_{z,0 \rightarrow 1} = 2\pi \times 5.90(2)$ kHz. The z -axis is perpendicular to the plane and points along the direction of gravity. In addition, we introduce a lattice in the plane with a spacing of $a = 680$ nm and a depth of $45E_r$ (trap frequency of 17 kHz), where $E_r = \hbar^2/8ma^2$ is the recoil energy of the effective lattice wavelength, with m the mass of ^{87}Rb . The resulting Mott insulator is at the focus of a high resolution optical imaging system capable of detecting atoms on individual lattice sites through fluorescence imaging. Light-assisted collisions at the start of the imaging process reduce the occupation of a site to its odd-even parity[21].

We start by demonstrating coherent driving of atoms in a Mott insulator between two orbitals. In the presence of a harmonic trap, the atoms in a 2D Mott insulator are arranged in concentric rings of fixed atom number per site, known as shells, with the largest occupation at the center[21]. We prepare a Mott insulator with two shells and modulate the axial lattice depth by $\pm 1.1(1)\%$ at a frequency chosen to transfer atoms from the ground state to the second excited orbital. A modulation frequency corresponding to exactly $\omega_{z,0 \rightarrow 2}$ is resonant for atoms in the outer shell with one atom per site ($n = 1$). Excitation to the fourth excited orbital is suppressed because of an energy shift of $\hbar \times 1200(80)$ Hz owing to the anharmonicity of the onsite potential. Rabi oscillations between the states $|g\rangle$ and $|e\rangle$ are detected by lowering

the axial lattice depth at the end of the modulation so that the excited orbital state becomes unbound and any population in it escapes along the z -axis due to gravity. The Rabi oscillations in that shell, shown in Fig. 2b, have a frequency $\Omega = 2\pi \times 23.3(2)$ Hz.

The OEB is demonstrated in the inner $n = 2$ shell by modulating at a frequency of $\omega_{z,0 \rightarrow 2} + (U_{ge} - U_{gg})/\hbar$. For our parameters, U_{gg} , U_{ge} , and U_{ee} are $h \times 480(30)$, $360(20)$, $310(20)$ Hz respectively. The Rabi oscillations between $|g, g\rangle$ and $1/\sqrt{2}(|e, g\rangle + |g, e\rangle)$ are detected as an oscillation of the parity between even and odd after ejecting the atom in the excited orbital and are shown in Fig. 2c. For the same modulation amplitude as before, the oscillations are expected to occur $\sqrt{2}$ times faster than the resonant oscillation in the $n = 1$ shell owing to Bose-enhancement[5]. We indeed observe a frequency ratio of 1.42(1) between the oscillation frequencies. A full frequency spectrum in the two shells is shown in Fig. 2a and the frequency separation of the two resonances of 160(10) Hz matches well with the theoretically expected value of 165(35) Hz when the impact of virtual orbital changing collisions is included (see Methods).

We next employ OEB to demonstrate a new path to cooling quantum gases. Evaporative cooling has been the workhorse technique for cooling atomic gases to nanokelvin temperatures. However, current interest in studying the physics of strongly-correlated materials, such as high- T_c cuprates, using ultracold gases[12, 13] has spurred research into developing new cooling techniques that can reach the requisite picokelvin regime[22, 23]. The field of quantum information offers an alternative cooling paradigm, wherein a sequence of unitary quantum gates purifies a subset of the qubits in a system by moving entropy and isolating it in another part of the system[10]. One realization of such a cooling scheme, heat-bath algorithmic cooling, has been successfully demonstrated with solid-state nuclear magnetic resonance qubits[11]. We introduce an analogous technique for quantum gases where the unitary operations are achieved using OEB, building on previous theoretical proposals in this direction[24–27].

A bosonic quantum gas at a finite temperature T adiabatically loaded into the ground band of a optical lattice stores its entropy in the form of atom number fluctuations in the zero-tunneling limit. Within the local density approximation, a lattice site with a local chemical potential μ is described by a density matrix $\hat{\rho} = \sum_n p_n |n\rangle\langle n|$, where p_n , the probability of having n atoms on the site, is given by $e^{-\beta(\frac{1}{2}U_{gg}n(n-1) - \mu n)}/Z$. Here, $\beta = 1/k_B T$ and Z is the grand canonical partition function. Cooling to zero temperature is achieved by changing the atom number distribution on each site to obtain $p_n = \delta_{n, \lceil \mu/U_{gg} \rceil}$.

The crucial ingredient for algorithmic cooling is a unitary operation that realizes the transformation $|n, m\rangle \rightarrow$

$|n-1, m+1\rangle$ for each n separately, where $|n, m\rangle$ denotes a Fock state with n atoms in the ground band and m atoms in an excited band. Resonant lattice modulation in the presence of OEB results in a rotation gate $\hat{R}_{nm}(t) = \exp[i(\Omega_{nm}t|n-1, m+1\rangle\langle n, m| + c.c.)]$, where Ω_{nm} is the transition's Rabi frequency and the required transformation is achieved for a modulation time $t = \pi/2\Omega_{nm}$. Entropy is transferred from the ground band to the excited band by performing a sequence of π gates $\hat{R}_{N-s,s}$ from $s = 0$ to $s = N-1$ with N chosen large enough such that $p_N \approx 0$ in the initial state. At the end of this sequence, most of the entropy of the gas has been transferred to the excited band and can be removed from the system by ejecting the atoms in that band. The local chemical potential μ is readjusted to recover a situation closer to thermal equilibrium by reducing the harmonic confinement to a new value ω_{low} so that $\mu < U_{gg}$ throughout the gas. At this point, residual entropy is stored in the resulting $n = 1$ Mott insulator in the form of holes that are preferably located near the edge of the cloud. The gas is allowed to rethermalize by lowering the lattice depth to allow tunneling, and the final entropy of the thermalized state would be significantly reduced compared to the initial state.

We start by experimentally demonstrating the algorithm on a state with known atom number, namely a four shell Mott insulator, and reducing the site occupation everywhere in the insulator to a single atom per site. To increase the blockade energy for this set of experiments, we transfer atoms to the fourth axial orbital rather than the second. We also replace the rotation gates demonstrated in the first part of this work with Landau-Zener transitions to improve the fidelity of the algorithm. We linearly sweep the modulation frequency from 20.90 kHz to 21.65 kHz in 250 ms. The chirp realizes a sequence of quantum operations that transfer atoms to the excited orbital one at a time, until only one atom remains in the ground state in all shells (Fig. 3a). We probe the ground orbital occupancy at different points in the frequency chirp by ejecting atoms in the higher orbital as before and then performing the parity imaging. The parity of the different shells during the chirp is shown in Fig. 4a, and an analogue of the typical Coulomb blockade staircase is seen in the data. Shell-sensitive manipulation of a Mott insulator had been achieved in previous experiments using a microwave transition between hyperfine states, but the lack of a strong blockade allowed transfer of only a small fraction of the population to the target state[28].

Next, we demonstrate cooling by performing the algorithm on a state that is far from the many-body ground state. To prepare such a state, we non-adiabatically load a condensate into a deep lattice, projecting the wavefunction onto a state with Poissonian site occupancy that rapidly loses coherence between sites. Using the same operation sequence as before, we progressively reduce the

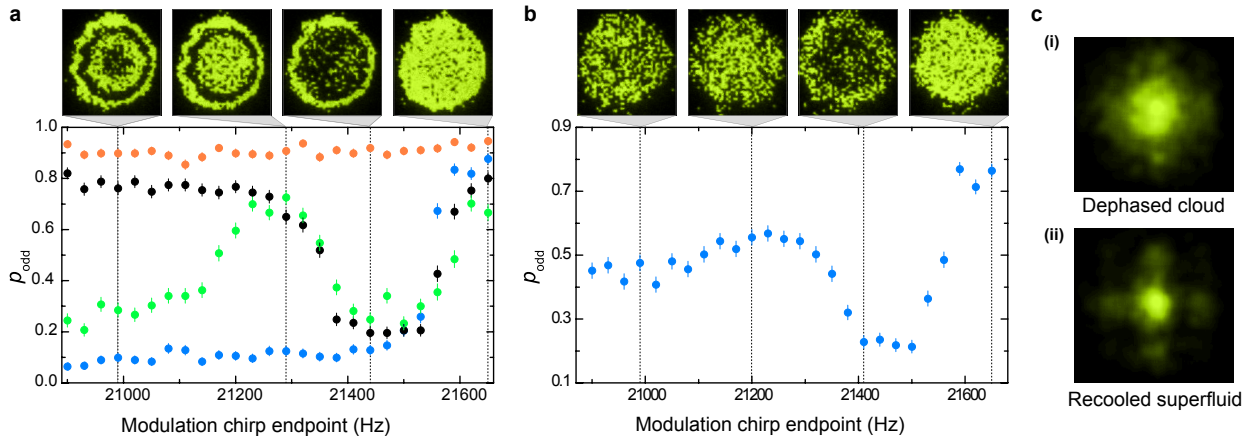


FIG. 4. Experimental realization of algorithmic cooling. **a**, By chirping the modulation towards higher frequencies, atoms in a four-shell Mott insulator are sequentially excited one at a time to the fourth orbital. Population in the higher orbital is subsequently ejected at the end of the chirp. The average parity in the $n = 1$ (orange), $n = 2$ (blue), $n = 3$ (black) and $n = 4$ (green) shell is shown at different points in the chirp, together with single shot images, illustrating the conversion to a three, two and finally one shell insulator. **b**, The same frequency chirp algorithmically cools a state with random occupancy into an $n = 1$ Mott insulator, observed as an enhancement in odd occupancy. All error bars are one standard error of the mean. **c**, (i) An incoherent cloud does not exhibit an interference pattern in a 5 ms time of flight expansion after adiabatically lowering the lattice depth. (ii) Cooling converts the incoherent cloud to a Mott insulator in the deep lattice. After adiabatically lowering the lattice depth, a superfluid forms and an interference pattern is obtained in the expansion images.

randomness of the ground band occupancy, preparing a single-occupancy Mott insulator (Fig. 3b). We enhance the odd occupancy from 0.45(1) to 0.76(2) (Fig. 4b), demonstrating significant atom number squeezing limited by the conversion efficiency of the Landau-Zener transitions. To complete the algorithm, we readjust the harmonic confinement to obtain a state close to the many-body ground state. We verify the ground state character by ramping back adiabatically to a $5E_r$ lattice in 100 ms and releasing the atoms from the lattice. Without cooling, we obtain a featureless cloud shown in Fig. 4c(i), indicating an absence of the coherence expected in the superfluid ground state. With cooling, the Mott insulator is adiabatically converted to a superfluid, giving rise to matter wave interference peaks shown in Fig. 4c(ii).

We now discuss the limits on the entropies that can be achieved with algorithmic cooling. The conversion efficiency to a single-occupancy Mott insulator is technically limited in our system by heating due to spontaneous emission during the sweep and to a lesser extent, by the efficiency of the Landau-Zener sweep for clouds with large average occupancies (see Methods). While we have demonstrated cooling of hot clouds, the single-occupancy probability we have achieved using algorithmic cooling in a two-shell Mott insulator is 0.94(1). This is comparable to what had been previously achieved with evaporative cooling, corresponding to an average entropy of $0.27k_B$ per particle [21]. Nevertheless, lattice heating can be made negligible by using a further-detuned lattice (e.g. 1064 nm), while shaped pulses can improve the Landau-Zener transfer efficiency[25]. More fundamentally, the

single-shot cooling algorithm we have implemented is limited by initial holes in the Mott insulator which cannot be corrected. However, repeated iterations of the algorithm can circumvent this problem and bring the cloud to zero entropy with quick convergence[25]. The cycle alternates between (a) using OEB to produce a reduced entropy $n = 1$ insulator in a harmonic confinement ω_{low} (demonstrated above) and (b) adiabatically increasing the confinement to ω_{high} in the presence of tunneling to move hot particles to the center of the cloud where they can be removed again. Alternatively, the outer edge of the cloud containing the holes can be removed using the high resolution available in our system[29].

In conclusion, we have observed a new blockade phenomenon in optical lattices when exciting atoms to higher orbitals, analogous to dipole excitation blockade in Rydberg atoms. The blockade permits deterministic manipulation of atom number in an optical lattice. We have used it to convert a multi-shell Mott insulator into a singly-occupied insulator with over a thousand sites, the largest quantum register achieved so far in an addressable system. The same technique allows initialization of registers in longer wavelength lattices where a Mott insulator cannot be prepared [30]. OEB also opens a route to implementing quantum gates in optical lattices. Single-site addressing[29], possible with our microscope, can perform rotations of individual orbital-encoded qubits rather than the global rotations demonstrated in this work. Controlled-NOT gates can be implemented by conditionally moving the control qubit onto the target qubit site, and performing an interaction-sensitive ro-

tation of the target qubit[14]. Finally, the algorithmic cooling technique we have developed could potentially achieve the ultralow entropies required for quantum simulation [12, 13] and computation in optical lattices, and establishes a bridge to quantum information for importing novel ideas for cooling quantum gases.

We would like to thank S. Fölling for stimulating discussions. This work was supported by grants from the Army Research Office with funding from the DARPA OLE program, an AFOSR MURI program, and by grants from the NSF.

-
- [1] H. Grabert and M. H. Devoret, eds., *Single charge tunneling: Coulomb blockade phenomena in nanostructures*, 1st ed. (Springer, 1992).
 - [2] K. Ono, D. G. Austing, Y. Tokura, and S. Tarucha, *Science* **297**, 1313 (2002).
 - [3] P. Cheinet, S. Trotzky, M. Feld, U. Schnorrberger, M. Moreno-Cardoner, S. Fölling, and I. Bloch, *Phys. Rev. Lett.* **101**, 090404 (2008).
 - [4] E. Urban, T. A. Johnson, T. Henage, L. Isenhowe, D. D. Yavuz, T. G. Walker, and M. Saffman, *Nat. Phys.* **5**, 110 (2009).
 - [5] A. Gaëtan, Y. Miroshnychenko, T. Wilk, A. Chotia, M. Viteau, D. Comparat, P. Pillet, A. Browaeys, and P. Grangier, *Nat. Phys.* **5**, 115 (2009).
 - [6] K. M. Birnbaum, A. Boca, R. Miller, A. D. Boozer, T. E. Northup, and H. J. Kimble, *Nature* **436**, 87 (2005).
 - [7] M. A. Kastner, *Rev. Mod. Phys.* **64**, 849 (1992).
 - [8] L. Isenhowe, E. Urban, X. L. Zhang, A. T. Gill, T. Henage, T. A. Johnson, T. G. Walker, and M. Saffman, *Phys. Rev. Lett.* **104**, 010503 (2010).
 - [9] T. Wilk, A. Gaëtan, C. Evellin, J. Wolters, Y. Miroshnychenko, P. Grangier, and A. Browaeys, *Phys. Rev. Lett.* **104**, 010502 (2010).
 - [10] P. Boykin, T. Mor, V. Roychowdhury, F. Vatan, and R. Vrijen, *Proc. Natl. Acad. Sci.* **99**, 3388 (2002).
 - [11] J. Baugh, O. Moussa, C. Pyan, A. Nayak, and R. Laflamme, *Nature* **438**, 470473 (2005).
 - [12] M. Lewenstein, A. Sanpera, V. Ahufinger, B. Damski, A. Sen, and U. Sen, *Adv. Phys.* **56**, 243 (2007).
 - [13] I. Bloch, J. Dalibard, and W. Zwerger, *Rev. Mod. Phys.* **80**, 885 (2008).
 - [14] P. Schneider and A. Saenz, (2011), cond-mat/1103.4950.
 - [15] D. Jaksch, C. Bruder, J. I. Cirac, C. W. Gardiner, and P. Zoller, *Phys. Rev. Lett.* **81**, 3108 (1998).
 - [16] M. Greiner, O. Mandel, T. Esslinger, T. W. Hänsch, and I. Bloch, *Nature* **415**, 39 (2002).
 - [17] T. Müller, S. Fölling, A. Widera, and I. Bloch, *Phys. Rev. Lett.* **99**, 200405 (2007).
 - [18] S. Will, T. Best, U. Schneider, L. Hackermüller, D. Lühmann, and I. Bloch, *Nature* **465**, 197 (2010).
 - [19] G. Wirth, M. Ölschläger, and A. Hemmerich, *Nat. Phys.* **7**, 147 (2011).
 - [20] P. Soltan-Panahi, J. Struck, P. Hauke, A. Bick, W. Plenkers, G. Meineke, C. Becker, P. Windpassinger, M. Lewenstein, and K. Sengstock, *Nature Phys.* **7**, 434 (2011).
 - [21] W. S. Bakr, A. Peng, M. E. Tai, R. Ma, J. Simon, J. I.

Gillen, S. Fölling, L. Pollet, and M. Greiner, *Science* **329**, 547 (2010).

- [22] D. C. McKay and B. DeMarco, *Rep. Prog. Phys.* **74**, 054401 (2011).
- [23] P. Medley, D. M. Weld, H. Miyake, D. E. Pritchard, and W. Ketterle, *Phys. Rev. Lett.* **106**, 195301 (2011).
- [24] P. Rabl, A. J. Daley, P. O. Fedichev, J. I. Cirac, and P. Zoller, *Phys. Rev. Lett.* **91**, 110403 (2003).
- [25] M. Popp, J.-J. Garcia-Ripoll, K. G. Vollbrecht, and J. I. Cirac, *Phys. Rev. A* **74**, 013622 (2006).
- [26] G. M. Nikolopoulos and D. Petrosyan, *J. Phys. B* **43**, 131001 (2010).
- [27] J. F. Sherson and K. Mølmer, (2010), cond-mat/1012.1457.
- [28] G. K. Campbell, J. Mun, M. Boyd, P. Medley, A. E. Leanhardt, L. G. Marcassa, D. E. Pritchard, and W. Ketterle, *Science* **313**, 649 (2006).
- [29] C. Weitenberg, M. Endres, J. F. Sherson, M. Cheneau, P. Schauß, T. Fukuhara, I. Bloch, and S. Kuhr, *Nature* **471**, 319 (2011).
- [30] K. D. Nelson, X. Li, and D. Weiss, *Nature Phys.* , 556 (2007).

METHODS

State Preparation

Our experiments begin with a degenerate 2D Bose gas of ^{87}Rb atoms prepared in the $|F = 1, m_f = -1\rangle$ state in a single layer of a 1D optical lattice with spacing $1.5 \mu\text{m}$, in the focal plane of a high resolution imaging system as described in previous work. The atoms are then loaded into a 2D optical lattice with spacing 680 nm , which is ramped up to a depth of $45E_r$ adiabatically on either a single- or many- body timescale, depending upon the experiment to be performed.

Higher Band Removal

The orbital blockade is observed through the deterministic removal of atoms in higher bands of the $1.5 \mu\text{m}$ lattice. For removal of atoms from the second band, this is achieved by reducing the depth of this lattice to 3.8 kHz from an initial depth of 35.8 kHz . Gravity produces a shift of 3.2 kHz per well, thus inducing second band atoms to Zener tunnel away within a few ms. The Landau-Zener tunneling rate from the ground state is given by $\Gamma_{LZ} = \frac{mga}{2\pi\hbar} e^{-g_c/g} \approx 12 \text{ Hz}$. Here g is the gravitational acceleration and $g_c = a\omega_z^2/4$. This effect leads to a loss of ground state atoms on the percent level, but can be made negligible by using excitations to the fourth band.

$\Delta\omega_z/2\pi$ [Hz]	$n = 1$	$n = 2$	$n = 3$	$n = 4$
$m = 0$	0	-217	-434	-651
$m = 1$	-9	-226	-443	
$m = 2$	-18	-235		
$m = 3$	-27			

TABLE I. Frequency shifts in Hz for a transition transferring an atom from the ground band to the fourth band, starting with n and m atoms in each of these bands. The shifts are measured relative to an initial state with one atom in the ground band and none in the excited band.

Band Dependent Energy Shifts

Due to its large spacing, the $1.5 \mu\text{m}$ lattice has a recoil energy of only 250 Hz. Consequently its depth is ~ 150 recoils, and its low-lying eigenstates are, to good approximation, the Hermite-Gaussians of a harmonic oscillator. The interaction energy between particles in bands m and n may thus be written in terms of the ground band interaction energy U_{00} as:

$$U_{nm} = U_{00}(2 - \delta_{nm}) \frac{\int |\psi_m(x)|^2 |\psi_n(x)|^2 dx}{\int |\psi_0(x)|^4 dx}$$

where $\psi_m(x)$ is the normalized m th harmonic oscillator wavefunction. The total interaction shift for M particles in band m , and N particles in band n is thus:

$$\frac{M(M-1)}{2} U_{mm} + \frac{N(N-1)}{2} U_{nn} + MNU_{mn}.$$

The interactions also produce off-resonant band changing collisions, with a Rabi frequency:

$$\Omega_{mn\leftrightarrow pq} = U_{00} C_{mn\leftrightarrow pq} \frac{\int \psi_m(x) \psi_n(x) \psi_p^*(x) \psi_q^*(x) dx}{\int |\psi_0(x)|^4 dx}$$

up to a combinatoric factor $C_{mn\leftrightarrow pq}$ resulting from Bose enhancement. For an energy defect of $\delta_{mn\leftrightarrow pq} \gg \Omega_{mn\leftrightarrow pq}$, this process produces an energy shift of $\Delta_{mn} = -|\Omega_{mn\leftrightarrow pq}|^2 / \delta_{mn\leftrightarrow pq}$. For our experiment, the dominant band changing collision is $|m = 0, n = 2\rangle \rightarrow |p = 1, q = 1\rangle$ with a Rabi frequency $\Omega_{02\leftrightarrow 11} = 2\pi \times 120$ Hz. In this case lattice anharmonicity and interaction shifts produce an energy defect of $\delta_{02\leftrightarrow 11} = 2\pi \times 330$ Hz, resulting in an additional overall shift of the $|0, 2\rangle$ state of $\Delta_{02} = -2\pi \times 45$ Hz.

Limits on entropies achievable with algorithmic cooling

In our system, the main limitation on the achievable entropies with algorithmic cooling is losses during the Landau-Zener chirp. Spontaneous emission after absorption of photons from the lattice leads to excitation of atoms from the ground state at a rate of 0.1 s^{-1} . These atoms are quickly lost due to tunneling in the higher bands in the case of the in-plane lattice or in the band filtering step in the case of the axial lattice. This leads to holes in an $n = 1$ Mott insulator (3% during the 250 ms ramp), setting a lower bound on the reachable entropy after thermalization of $\approx 0.15 k_B$ per particle. The lattice light is detuned 25 nm to the blue of the atomic resonance, and the heating rate can be made negligible by increasing the detuning (e.g. using 1064 nm lattice light). A more fundamental limit on the single-shot cooling algorithm demonstrated here is given by initial holes in the Mott insulator that cannot be corrected. For our Mott insulators, the hole fraction is on the order of 0.5% corresponding to a post-thermalization entropy of $\approx 0.06 k_B$ per particle. This limit can be overcome by the iterative algorithm described in the text. For Mott insulators with large initial atom numbers per site, it is also important to take into account the efficiency of the Landau-Zener chirp. For excitation to the second band, the measured efficiency is $0.94(1)$.